

# Wing patterning gene redefines the mimetic history of *Heliconius* butterflies

Heather M. Hines<sup>a,1</sup>, Brian A. Counterman<sup>b</sup>, Riccardo Papa<sup>c</sup>, Priscila Albuquerque de Moura<sup>d</sup>, Marcio Z. Cardoso<sup>d</sup>, Mauricio Linares<sup>e</sup>, James Mallet<sup>f,g</sup>, Robert D. Reed<sup>h</sup>, Chris D. Jiggins<sup>i</sup>, Marcus R. Kronforst<sup>j</sup>, and W. Owen McMillan<sup>a,k</sup>

<sup>a</sup>Department of Genetics, North Carolina State University, Raleigh, NC 27695; <sup>b</sup>Department of Biological Sciences, Mississippi State University, Mississippi State, MS 39762; <sup>c</sup>Department of Biology and Center for Applied Tropical Ecology and Conservation, University of Puerto Rico-Rio Piedras, Rio Piedras, Puerto Rico PR 00931; <sup>d</sup>Departamento de Botânica, Ecologia e Zoologia, Universidade Federal do Rio Grande do Norte, Natal RN 59072-970, Brazil; <sup>e</sup>Facultad de Ciencias Naturales y Matemáticas, Universidad del Rosario, Carrera 24 No. 63c-69, Bogotá Colombia; <sup>f</sup>Department of Genetics, Evolution and Environment, University College London, London, WC1E 6BT United Kingdom; <sup>g</sup>Department of Organismal and Evolutionary Biology, and <sup>h</sup>Faculty of Arts and Sciences Center for Systems Biology, Harvard University, Cambridge MA 02138; <sup>i</sup>Department of Ecology and Evolutionary Biology, University of California, Irvine, CA 92697; <sup>j</sup>Department of Zoology, University of Cambridge, Cambridge CB2 3EJ, United Kingdom; and <sup>k</sup>Smithsonian Tropical Research Institute, Apartado Postal 2072, Balboa, Panama

Edited by May R. Berenbaum, University of Illinois at Urbana-Champaign, Urbana, IL, and approved October 12, 2011 (received for review June 22, 2011)

The mimetic butterflies *Heliconius erato* and *Heliconius melpomene* have undergone parallel radiations to form a near-identical patchwork of over 20 different wing-pattern races across the Neotropics. Previous molecular phylogenetic work on these radiations has suggested that similar but geographically disjunct color patterns arose multiple times independently in each species. The neutral markers used in these studies, however, can move freely across color pattern boundaries, and therefore might not represent the history of the adaptive traits as accurately as markers linked to color pattern genes. To assess the evolutionary histories across different loci, we compared relationships among races within *H. erato* and within *H. melpomene* using a series of unlinked genes, genes linked to color pattern loci, and *optix*, a gene recently shown to control red color-pattern variation. We found that although unlinked genes partition populations by geographic region, *optix* had a different history, structuring lineages by red color patterns and supporting a single origin of red-rayed patterns within each species. Genes closely linked (80–250 kb) to *optix* exhibited only weak associations with color pattern. This study empirically demonstrates the necessity of examining phenotype-determining genomic regions to understand the history of adaptive change in rapidly radiating lineages. With these refined relationships, we resolve a long-standing debate about the origins of the races within each species, supporting the hypothesis that the red-rayed Amazonian pattern evolved recently and expanded, causing disjunctions of more ancestral patterns.

Müllerian mimicry | population genetics | phylogeography

Researchers typically rely on neutrally evolving loci to generate a phylogenetic and population genetic history of adaptive divergence. The rationale is that these markers provide an unbiased view of the relationships among divergent phenotypes and a better understanding of the evolutionary processes generating variation. However, the genome is a complicated mosaic shaped by an interplay of mutation, drift, selection, and recombination. Recombination allows different regions of the genome to experience alternative restrictions to gene flow, and thus develop different evolutionary trajectories. The closer a genetic marker is to the alleles responsible for adaptive differences, the more likely that it will trace the history of phenotypic change.

Understanding how phenotypic variation is generated in nature is greatly enhanced by studying groups that are actively undergoing diversification. By deciphering the history of such diverse phenotypes we gain a clearer understanding of the evolutionary process, including the tempo and mode of phenotypic change. *Heliconius* butterflies present one of the most striking examples of a recent phenotypic radiation. The 40 species in the genus exhibit hundreds of wing patterns that are involved in Müllerian mimicry complexes, where distasteful species converge on a shared warning signal to avoid predation. This convergence is particularly remarkable in two species, *Heliconius erato* and *Heliconius melpomene*. These

species are phylogenetically distant and do not hybridize (1), yet they have converged to share over 20 different mimetic color patterns across the Neotropics (Fig. 1) (2, 3). Most of the color-pattern diversity in these species can be partitioned into two major groups: “rayed” patterns, involving orange-red rayed hindwing patterns with orange-red basal forewings, and “red-banded” patterns, involving crimson-banded forewings and hindwings that are black and may have a yellow bar (Fig. 1). The rayed phenotypes are comimetic with several other *Heliconius* species across a broad contiguous Amazonian distribution. In contrast, the red-banded phenotypes are mostly restricted to just the two comimics *H. erato* and *H. melpomene*, and are found in multiple disjunct regions around the periphery of the Amazon.

A long history of research has been devoted to understanding the historical processes generating the wing pattern diversity within *H. erato* and *H. melpomene*. Earlier investigators proposed an allopatry-based Pleistocene refugium hypothesis to explain these patterns, whereby the identical patchwork of color patterns that characterize *H. erato* and *H. melpomene* arose simultaneously when populations of the two species became isolated together in forest refugia during Pleistocene cooling (2–4). Mallet proposed an alternative parapatric-based hypothesis, where color patterns evolved through a process similar to Wright’s shifting balance (5). Under his hypothesis, novel color patterns became common enough locally to be fixed by frequency dependent selection. If advantageous, the pattern would spread, resulting in shifting of the boundaries of mimicry complexes over time (6, 7). Mallet proposed that the disjunct color patterns we see today may have had a single origin and been created when a rayed pattern originated and spread from the Amazon, displacing and fragmenting a previously contiguous red-banded population (8).

As a test of these hypotheses, molecular markers unlinked to color pattern, including mtDNA (9–11), nuclear sequences (12), and amplified fragment length polymorphism (AFLPs) (11), have been used to more carefully dissect the timing of the two parallel radiations and the relationships among color pattern races within the two comimics. These studies inferred an older (10–12) and different phylogenetic history for *H. erato* than

Author contributions: H.M.H., B.A.C., R.D.R., C.D.J., M.R.K., and W.O.M. designed research; H.M.H., B.A.C., R.P., and W.O.M. performed research; P.A.d.M., M.Z.C., M.L., C.D.J., and M.R.K. contributed new reagents/analytic tools; H.M.H., B.A.C., and W.O.M. analyzed data; H.M.H., B.A.C., R.P., J.M., R.D.R., C.D.J., M.R.K., and W.O.M. wrote the paper.

The authors declare no conflict of interest.

This article is a PNAS Direct Submission.

Data deposition: The sequences reported in this paper have been deposited in the GenBank database (accession nos. JN897400 and JN898803) and in the Dryad database (doi:10.5061/dryad.8h154h65).

<sup>1</sup>To whom correspondence should be addressed. E-mail: heather\_hines@ncsu.edu.

This article contains supporting information online at [www.pnas.org/lookup/suppl/doi:10.1073/pnas.1110096108/-DCSupplemental](http://www.pnas.org/lookup/suppl/doi:10.1073/pnas.1110096108/-DCSupplemental).



**Table 1. Population structure inferred from AMOVA and phylogenetic signal in color pattern**

Gene	Type (kb)	AMOVA: population structure				Phylogeny		CP Steps*
		Color pattern		Geography		Color pattern: Amazon		
		% Var	P value	% Var	P value	% Var	P value	
<i>H. erato</i>								
<i>optix</i>	Target (0)	55.19	0.0010	21.70	0.0675	52.51	0.0147	3
<i>kinesin</i>	Linked (-181)	8.19	0.0323	7.84	0.0411	4.24	0.1281	14–18
<i>GPCR</i>	Linked (-172)	8.24	0.0547	26.37	0.0010	5.77	0.1017	17
<i>bves</i>	Linked (-220)	9.06	0.0147	2.53	0.1799	14.73	0.0284	12–20
<i>VanGogh</i>	Linked (+87)	-0.94	0.4135	7.98	0.0147	-3.95	0.9013	21
<i>SUMO</i>	Unlinked	-0.30	0.5591	0.94	0.0391	-1.29	0.9775	30
<i>Suzy</i>	Unlinked	-1.50	0.6305	0.15	0.2239	1.16	0.2160	24–33
<i>2654</i>	Unlinked	-0.19	0.4230	-1.33	0.7146	-0.65	0.5494	24–34
<i>CAT</i>	Unlinked	15.91	0.2102	72.14	0.0010	-1.54	0.9091	17–23
<i>mt</i>	Unlinked	20.09	0.0459	72.06	0.0010	-1.94	0.6090	8*
<i>H. melpomene</i>								
<i>optix</i>	Target	21.84	0.0147	31.67	0.0029	14.68	0.0557	5
<i>kinesin</i>	Linked	19.50	0.0381	18.40	0.0538	15.24	0.2307	4–18
<i>GPCR</i>	Linked	1.61	0.2893	3.94	0.0997	3.93	0.1144	7–28
<i>bves</i>	Linked	4.95	0.1965	34.80	0.0049	0.57	0.5572	11–27
<i>VanGogh</i>	Linked	3.37	0.1799	12.69	0.0156	10.50	0.0244	15–22
<i>SUMO</i>	Unlinked	-0.54	0.4438	12.89	0.0254	-6.89	0.8534	19–22
<i>Suzy</i>	Unlinked	-4.04	0.5093	32.10	0.0068	-6.58	0.6227	13–39
<i>2654</i>	Unlinked	1.87	0.2581	24.10	0.0020	1.32	0.3597	10–31
<i>CAT</i>	Unlinked	-0.84	0.4438	13.18	0.0117	-4.60	0.9707	21–24
<i>mt</i>	Unlinked	-0.51	0.3744	35.21	0.0078	-15.08	0.9306	13*

CP Steps represents the number of color-pattern changes inferred on the neighbor-joining trees using parsimony, with ranges representing alternative reconstruction of polytomies; Var, variance. Gray shading represents color pattern linked genes. Unshaded rows represent unlinked genes.

\*Because *mt* has only one haplotype for each individual, approximately half the number of steps are expected.

were structured mostly by geography. In *H. erato*, nucleotide variation at three (*2654*, *Suz12*, and *SUMO*) of the four unlinked nuclear markers was broadly distributed among populations with very little evidence of population structure among races, geographic regions, or color-pattern phenotypes in the analysis of molecular variance (AMOVA) (Table 1) or phylogenetic analyses (Fig. S1 H–J). In contrast, the mitochondrial fragment and the unlinked nuclear marker *CAT* had clear population structure, largely reflecting geography (Figs. 3A, Table 1, and Fig. S1G). Both genes recognized distinct lineages that match closely to the Amazonian, Caribbean, and Chacoan/Paranan biotic domains of Morrone (25) (Fig. 1). In the AMOVA, a large amount of variation in both of these genes was explained by geographic divisions into Amazon + Chacoan and Caribbean domains (72.1% each). A fair amount of variation was also explained by color pattern (rayed vs. nonrayed patterns; 15.9–20.1%). However, this pattern was likely the result of regional differences in color-pattern phenotypes, as rayed phenotypes are found only in the Amazon region (Fig. 1). When we reduce the effect of geographic structure by examining color-pattern structure within the Amazonian region, none of the genetic variation was explained by color pattern (Table 1).

In *H. melpomene*, there was a strong geographic pattern to the distribution of variation across unlinked loci. The mitochondrial fragment demarcated four major populations, including the same three lineages for *H. erato* (Amazon, Caribbean, and Chacoan/Parana) but it differed in resolving a Guiana Shield lineage consisting of Trinidad and French Guianan specimens (Figs. 3A and Fig. S1F). The unlinked nuclear markers have less straightforward phylogenetic clustering of populations (Figs. 3A and Fig. S1 G–J). However, all of these genes demonstrated significant geographic signal with a fair amount of variation explained by the geographic division of the Amazon+Chacoan from the Caribbean region (12.9–35.2%) in the AMOVA. These same genes exhibited virtually no variation that could be explained by color pattern (Table 1).

***optix* Exhibits Population Structure by Color Pattern.** In contrast to unlinked markers, *optix* showed strong population structure based on color pattern. This structure was most apparent in *H. erato*, where the Bayesian phylogeny (Fig. S1A), neighbor-joining tree (Fig. 3A), and haplotype network (Fig. 3B) of the inferred haplotypes for *optix* place nearly all haplotypes of rayed races into a single derived lineage. Over half of the *optix* variation was explained by color pattern phenotype (55.2%,  $P = 0.00098$ ), a much larger portion than any other gene (Table 1). This large and significant contribution of color pattern remained when the effect of geographic structure is removed (52.5%,  $P = 0.01466$ ).

There was less intraspecific variation in *optix* in *H. melpomene*, making phylogenetic and network inferences more difficult. Nonetheless, individuals clustered by color-pattern phenotype. In the Bayesian tree, most of the rayed phenotypes formed a basal polytomy (Fig. S1A). In contrast, the neighbor-joining tree clustered most of the rayed alleles together, but the alleles fell on a derived lineage. In the haplotype network (Fig. 3B) the rayed haplotypes clustered together near the origin of *H. melpomene*. AMOVA similarly supported color-pattern clustering in *optix* for *H. melpomene*. Using all populations, *optix* had the highest variation of any locus explained by color pattern (21.8%,  $P = 0.01466$ ). When removing the effect of geographic structure, the variation explained by color pattern structure for *optix* is reduced, but nearly significant (14.7%,  $P = 0.0557$ ). The inferred patterns of population structure for unlinked markers and *optix* were further supported by STRUCTURE analyses (SI Text and Fig. S2). Similar to every locus thus far examined, a neighbor-joining tree combining *optix* sequences for both *H. melpomene* and *H. erato* resulted in two distinct clades, with no sharing of alleles between the comimics (Fig. S1A).

There were a few exceptions to the complete clustering by color pattern in both the *H. erato* and *H. melpomene* *optix* data (Fig. 3B and Fig. S1A). In many of these exceptions, an individual possessed both a rayed and nonrayed haplotype. For example, three of the five *H. erato microclea* individuals possessed



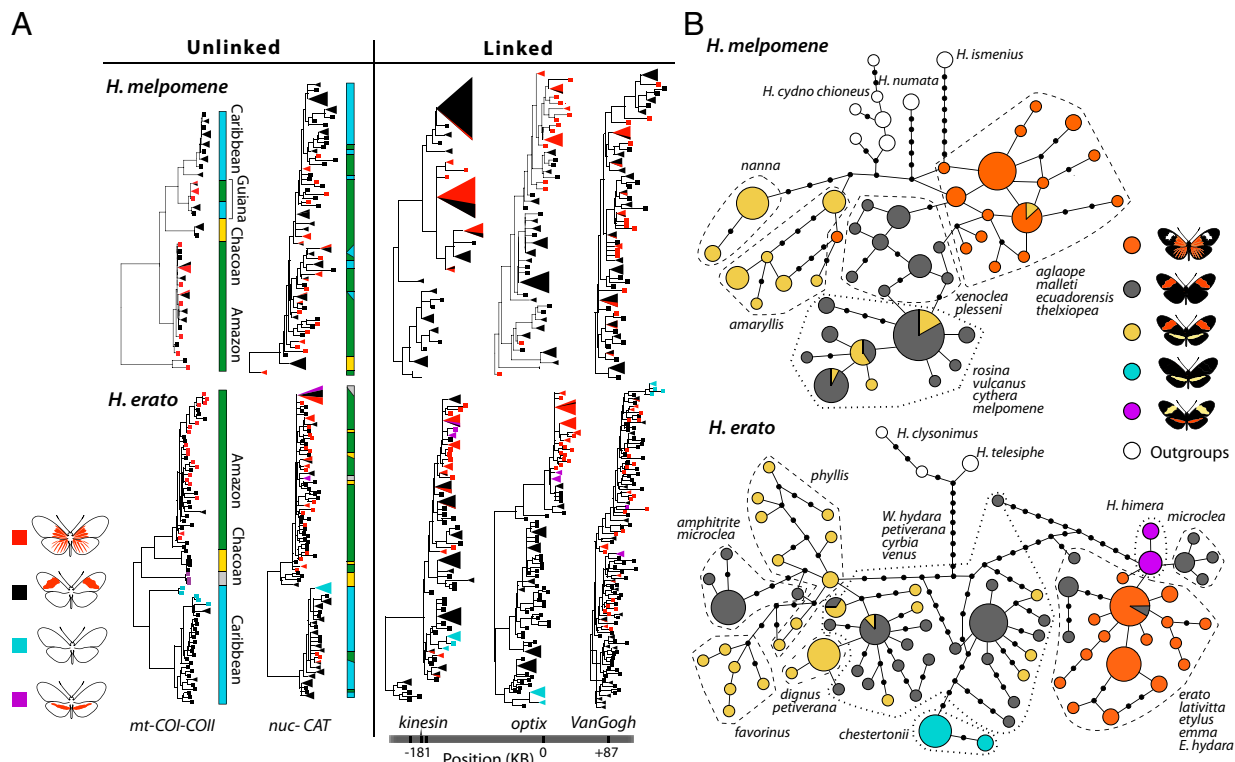


**Fig. 3.** Phylogeographic relationships of *H. erato* and *H. melpomene*. (A) Phylogenetic clustering of color pattern in select color-pattern linked and unlinked markers. Trees were constructed using neighbor-joining methods with terminal nodes colored by the major red color-pattern phenotypes. Unlinked markers displayed are those with greater population structure, and linked markers include *kinesin*, which has the greatest color pattern association besides *optix*, and the closest gene, *VanGogh*. Triangular clades represent shared haplotypes, with size reflecting the frequency of the haplotype. Colored bars indicate geographic distribution. (B) *optix* haplotype networks. Each node represents a haplotype, lines between nodes represent a single base change, and the size of the node represents haplotype frequency. Nodes are colored by the color patterns containing that haplotype. Major racial groups are indicated using dashed polygons, with dashes differing by geographic domain (large dash -, Amazon/Chacoan; small dash -, Caribbean).

the *H. melpomene* radiation may have originated and spread from the Amazon and colonized other regions of Central and South America, a finding consistent with results from large-scale AFLP data (10). Support for this hypothesis, however, is weak, and there is more variation within nonrayed phenotypes than rayed phenotypes. Furthermore, although patterns are not transferred between *H. erato* and *H. melpomene*, *H. melpomene* may have acquired different red pattern phenotypes through hybridization with its closest relatives. *H. melpomene* is a member of a larger complex of species that are known to hybridize in nature, including a number of species in the Amazon region with rayed phenotypes (1, 27). The acquisition of new color patterns by hybridization is thought to play an important role in the evolution of pattern variation in *Heliconius* (24, 28, 29). Additional sequence data around *optix* across the *H. melpomene* species-complex should help resolve the origins of red patterns within the *melpomene* group.

**Advergence and Convergence and the Origins of Mimicry Between *H. erato* and *H. melpomene*.** These data allow us to reassess hypotheses about the timing of the parallel coradiations and the origins of the mimetic relationship between *H. erato* and *H. melpomene*. Our data provide additional evidence against simultaneous diversification of *H. erato* and *H. melpomene*, but do not rule out the idea that the rayed patterns may have diverged more recently in parallel in the Amazon. Overall, *H. erato* harbors substantially more variation and has deeper intraspecific genealogies than *H. melpomene*. The two species are also inferred to have different phylogeographic history, with eastward spread of color pattern in *H. erato* and westward spread in *H. melpomene*. Although exact dating is difficult given that selection will impact rates of genetic divergence (16, 17), the discrepancies in timing and geographic pattern of the radiations appear to be driven mostly by the considerably older origins of the nonrayed *H. erato* patterns. Extant

levels of variation in *optix* and unlinked markers in rayed phenotypes are more similar between comimics, suggesting that rayed patterns diverged at about the same time in the two species. The parallel radiation can thus be explained by *H. erato* establishing the red-banded populations first, *H. melpomene* adverting on these patterns, and both species acquiring the Amazonian rayed mimetic pattern around the same time, with subsequent spread of this pattern fragmenting established red-banded populations. It is also possible that both *H. erato* and *H. melpomene* converged together on the rayed pattern to mimic other Amazonian heliconiines. Unlike the nonrayed forms of *H. erato* and *H. melpomene*, the rayed phenotypes are part of a larger mimicry complex composed of over a dozen species (mostly *Heliconius* but also other butterfly genera, and even day-flying moths) that share the same pattern (4, 13, 30). The deeper phylogenetic origins of this convergence can now be more thoroughly explored using the genes underlying the phenotypic change.

**Conclusions and Future Directions.** Nucleotide variation at regions tightly linked to the functional sites driving adaptive change provide unique insights into the origins of the patchwork of mimetic color pattern races in *H. erato* and *H. melpomene* that has intrigued biologists for over 150 y. Contrary to the history reflected in the majority of the genome, data around the functional sites driving phenotypic variation suggest that similar wing-pattern phenotypes share a common origin within each of the two parallel radiations. These data also suggest that the rayed Amazonian phenotype evolved recently and around the same time in *H. erato* and *H. melpomene*, and spread rapidly, replacing the ancestral red-banded phenotype. Although variation in red is a major aspect of the complex story of mimicry between *H. erato* and *H. melpomene*, a number of other loci interact with the red locus to generate the phenotypic variation that characterizes the

two radiations. Current research is identifying these loci, including loci that modulate the shape of the forewing band and the presence of a yellow hindwing bar (21). A combination of sequence information across the different color-pattern loci promises an even more complete picture of the history of these coradiations and a deeper understanding about how novel variation arises and spreads during adaptive change.

## Materials and Methods

**Taxonomic Sampling and DNA Data Collection.** We sequenced 137 individuals of *H. erato* (including three *Heliconius himera*) and *H. melpomene*, and two outgroups for each species (Fig. 1 and Table S1). Specimens were sequenced for 10 gene fragments, including four unlinked nuclear markers [*CAT* (1081 bp), *SUMO* (805 bp), *Suz12* (520 bp), *Gene 2654* (872 bp)], a mitochondrial region *COI-tRNA<sup>Leu</sup>-COII* (1,510 bp), and five genes within the red color-pattern interval. These genes included an 800-bp *optix* transcript (432 bp of coding sequence and 361–370 bp of 3' UTR) and coding regions of four genes within 250 kb of *optix* (Table 1), including *kinesin* (501 bp), *GPCR* (522 bp), *VanGogh* (715 bp), and *bves* (385 bp). Further gene information is available in Table 1 and Table S4.

DNA was extracted from thoracic tissue using the Qiagen DNA Plant kit, PCR-amplified (Table S4), and purified using ExoSAP-IT (USB, Affymetrix). We sequenced both forward and reverse strands using ABI Big Dye Terminator v3.1 reactions and PCR primers, and called SNPs based on consistent double peaks in chromatograms. For *optix*, we cloned (TOPO TA Cloning kit; Invitrogen) a few individuals (Table S1) to facilitate phasing. Haplotypes were inferred from polymorphic sequences using PHASEv2.1 (31), allowing recombination (32) with a recombination rate prior of 0.04, and declaring known phases from cloned individuals.

**Reconstructing Phylogenetic Trees and Haplotype Networks.** We constructed neighbor-joining trees of phased haplotypes for each gene and species in PAUP\* 4.0b10 (33). We also performed a combined neighbor-joining analysis on *optix* for the two species to test for allele sharing. For *optix* and *mt COI-COII* we constructed Bayesian phylogenies of haplotypes using MrBayes v.3.1.2 (34)

(Fig. S1). We generated parsimony-based haplotype networks for *optix* using TCS 1.2.1 (35), relaxing the number of steps to allow placement of outgroups.

**Tests for Population Structure.** We inferred population structure for each gene and species using an AMOVA implemented in Arlequin 3.1 (36). Population structure was assessed relative to geographic region (Caribbean, Amazon +Chacoan) (Fig. 1 and Table S1), color pattern (rayed, nonrayed), and race within these groups by comparing variance in uncorrected genetic distances of phased haplotypes. Outgroups, *H. himera* and *H. erato chesteronii* were excluded, as these lineages show strong reproductive isolation from other races. We also assigned individuals to populations based on Hardy–Weinberg equilibrium assumptions using STRUCTURE 2.2 (37) (SI Text). As a phylogenetic measure of color-pattern signal for each gene, we inferred the number of evolutionary steps between rayed and nonrayed color patterns using parsimony-based character reconstruction on neighbor-joining trees in MacClade (38).

**Genetic Diversity and Recombination Estimates.** Methods for estimating genetic diversity and recombination are outlined in Tables S2 and S3. Mismatches (nucleotide differences) between pairs of haplotypes were calculated within species and within rayed and red-banded sets (Table S1) of individuals using concatenated sequences of the nuclear unlinked genes for each individual in Arlequin 3.1.

**ACKNOWLEDGMENTS.** We thank Stephanie Ruzsa, Vincent Izzi, Nicola Chamberlain, and Felix Araujo-Perez for assistance with sample preparation and sequencing; Matt Bertone for graphics assistance; Jeff Thorne for analytical advice; and the Peruvian Ministerio de Agricultura and Instituto Nacional De Recursos Naturales (004-2008-INRENA-IFF5-DCB and 011756-AG-INRENA), the Ecuadorian Ministerio del Ambiente Ecuadoriano (013-09 IC-FAU-DNB/MA), and the Brazilian Ministério do Meio Ambiente (permit 10894-1) for collection permits. This work was funded by a Ruth L. Kirschstein National Research Service Award F32 GM889942 (to H.M.H.), Fapem/ Conselho Nacional de Pesquisas Grant PPP/2007 (to M.Z.C.); National Institutes of Health/National Institute of General Medical Sciences Grant GM068763 and National Science Foundation Division of Environmental Biology (DEB) Grant 1020355 (to M.R.K.); Biotechnology and Biological Sciences Research Council Grant G060903 (to J.M.); and National Science Foundation Grants DEB-0844244 and DEB-0715096 (to R.D.R. and W.O.M.).

- Mallet J, Beltrán M, Neukirchen W, Linares M (2007) Natural hybridization in heliconiine butterflies: The species boundary as a continuum. *BMC Evol Biol* 7:28.
- Brown KS, Sheppard PM, Turner JRG (1974) Quaternary refugia in tropical America: Evidence from race formation in *Heliconius* butterflies. *Proc R Soc Lond B Biol Sci* 187:369–378.
- Sheppard PM, Turner JRG, Brown KS, Benson WW, Singer MC (1985) Genetics and the evolution of Müllerian mimicry in *Heliconius* butterflies. *Philos Trans R Soc Lond, B* 308:433–613.
- Turner JRG (1983) Mimetic butterflies and punctuated equilibria: Some old light on a new paradigm. *Biol J Linn Soc Lond* 20:277–300.
- Wright S (1982) Character change, speciation, and the higher taxa. *Evolution* 36:427–443.
- Mallet J, Singer MC (1987) Individual selection, kin selection, and the shifting balance in the evolution of warning colours: The evidence from butterflies. *Biol J Linn Soc Lond* 32:337–350.
- Mallet J (2010) Shift happens! Shifting balance and the evolution of diversity in warning colour and mimicry. *Ecol Entomol* 35:90–104.
- Mallet J (1993) *Hybrid Zones and the Evolutionary Process*, ed Harrison RG (Oxford University Press, New York), pp 226–260.
- Brower AVZ (1994) Rapid morphological radiation and convergence among races of the butterfly *Heliconius erato* inferred from patterns of mitochondrial DNA evolution. *Proc Natl Acad Sci USA* 91:6491–6495.
- Brower AVZ (1996) Parallel race formation and the evolution of mimicry in *Heliconius* butterflies: A phylogenetic hypothesis from mitochondrial DNA sequences. *Evolution* 50:195–221.
- Quek S-P, et al. (2010) Dissecting comimetic radiations in *Heliconius* reveals divergent histories of convergent butterflies. *Proc Natl Acad Sci USA* 107:7365–7370.
- Flanagan NS, et al. (2004) Historical demography of Mullerian mimicry in the neotropical *Heliconius* butterflies. *Proc Natl Acad Sci USA* 101:9704–9709.
- Eltringham H (1917) On the specific and mimetic relationships of the genus *Heliconius*. *Trans Entomol Soc Lond* 1916:101–148.
- Turner JRG, Johnson MS, Eanes WF (1979) Contrasted modes of evolution in the same genome: Allozymes and adaptive change in *Heliconius*. *Proc Natl Acad Sci USA* 76:1924–1928.
- Mallet J, McMillan WO, Jiggins CD (1998) *Endless Forms: Species and Speciation*, ed Howard DJ (Oxford University Press, New York), pp 390–403.
- Counterman BA, et al. (2010) Genomic hotspots for adaptation: The population genetics of Müllerian mimicry in *Heliconius erato*. *PLoS Genet* 6:e1000796.
- Baxter SW, et al. (2010) Genomic hotspots for adaptation: The population genetics of Müllerian mimicry in the *Heliconius melpomene* clade. *PLoS Genet* 6:e1000794.
- Terai Y, Morikawa N, Okada N (2002) The evolution of the pro-domain of bone morphogenetic protein 4 (*Bmp4*) in an explosively speciated lineage of East African cichlid fishes. *Mol Biol Evol* 19:1628–1632.
- Colosimo PF, et al. (2005) Widespread parallel evolution in sticklebacks by repeated fixation of *Ectodysplasin* alleles. *Science* 307:1928–1933.
- Shapiro MD, et al. (2004) Genetic and developmental basis of evolutionary pelvic reduction in threespine sticklebacks. *Nature* 428:717–723.
- Joron M, et al. (2006) A conserved supergene locus controls colour pattern diversity in *Heliconius* butterflies. *PLoS Biol* 4:e303.
- Reed RD, et al. (2011) *optix* drives the repeated convergent evolution of butterfly wing pattern mimicry. *Science* 333:1127–1141.
- Nadeau NJ, et al. (2011) Evidence for genomic islands of divergence among hybridizing species and subspecies of *Heliconius* butterflies obtained by large-scale targeted sequencing. *Phil Trans Roy Soc B*, in press.
- Salazar C, et al. (2010) Genetic evidence for hybrid trait speciation in *Heliconius* butterflies. *PLoS Genet* 6:e1000930.
- Morrone JJ (2006) Biogeographic areas and transition zones of Latin America and the Caribbean islands based on panbiogeographic and cladistic analyses of the entomofauna. *Annu Rev Entomol* 51:467–494.
- Blum MJ (2002) Rapid movement of a *Heliconius* hybrid zone: Evidence for phase III of Wright's shifting balance theory? *Evolution* 56:1992–1998.
- Beltran M, Jiggins CD, Brower AVZ, Bermingham E, Mallet J (2007) Do pollen feeding, pupal-mating and larval gregariousness have a single origin in *Heliconius* butterflies? Inferences from multilocus DNA sequence data. *Biol J Linn Soc Lond* 92:221–239.
- Gilbert LE (2003) *Ecology and Evolution take Flight*, eds Boggs CL, Watt WB, Ehrlich PR (University of Chicago Press, Chicago), pp 281–318.
- Mallet J (2009) *Speciation and Patterns of Diversity*, eds Butlin R, Bridle J, Schluter D (Cambridge University Press, Cambridge, U.K.; New York), pp 177–194.
- Mallet J (2001) Causes and consequences of a lack of coevolution in Müllerian mimicry. *Evol Ecol* 13:777–806.
- Stephens M, Smith NJ, Donnelly P (2001) A new statistical method for haplotype reconstruction from population data. *Am J Hum Genet* 68:978–989.
- Li N, Stephens M (2003) Modeling linkage disequilibrium, and identifying recombination hotspots using single-nucleotide polymorphism data. *Genetics* 165:2213–2233.
- Swofford DL (2002) *PAUP\*. Phylogenetic Analysis Using Parsimony (\*and Other Methods)*, Version 4 (Sinauer Associates, Sunderland, Massachusetts).
- Ronquist F, Huelsenbeck JP (2003) MrBayes 3: Bayesian phylogenetic inference under mixed models. *Bioinformatics* 19:1572–1574.
- Clement M, Posada D, Crandall KA (2000) TCS: A computer program to estimate gene genealogies. *Mol Ecol* 9:1657–1659.
- Excoffier LGL, Schneider S (2005) Arlequin ver. 3.0: An integrated software package for population genetics data analysis. *Evol Bioinform Online* 1:47–50.
- Pritchard JK, Stephens M, Donnelly P (2000) Inference of population structure using multilocus genotype data. *Genetics* 155:945–959.
- Maddison DR, Maddison WP (2005) *MacClade 4.08* (Sinauer, Sunderland, MA).